CFD Modeling of flow through S-Shaped Duct

Md. Nadim Shams[1], Raj Kumar Singh[2], Md. Zunaid[3]

[1]JK Laxmipat University, Jaipur, Rajasthan, India
[2, 3] Delhi Technological University, Bawana Road, Delhi, India

Abstract : This Paper investigates the flow inside an S- Shaped square Duct. In this paper, a computational fluid dynamics (CFD) model of fully developed turbulent flow(k-ϵ model) is implemented with the help of FLUENT software and the variation of pressure along the length of bend with variation in Reynolds number is analyzed. The curvatures is investigated at Reynolds numbers Re=$4.73x10^4$ and $1.47x10^5$. A non-dimensional parameter ω, defined as the total pressure loss coefficient is analyzed for finding out the total pressure loss in the duct. Cp Data obtained from the simulation of S-shaped ducts show that there is flow separation at the near side wall of the first bend and far side wall of the second bend. At high Reynolds number separation is more dominant near junction of bend as compare to low Reynolds number flow. To improve the flow in S-ducts, vortex generators as flow control methods is implemented. This methods shown to be effective in suppressing flow separation and reducing total pressure loss.

***Keywords*:** CFD, FLUENT, Reynolds number, S- Shaped square Duct, Vortex generators

I. INTRODUCTION

The layout of any practical piping system necessarily includes bends and the accurate prediction of pressure losses, flow rate and pumping requirements demands knowledge of the character of curved duct flows, such wide applications in the industry have forced researchers to acknowledge the importance of study of flow in curved ducts.

Curved duct flows are common in aerospace applications. Many military aircraft have wing root or ventral air intakes and the engine is usually positioned in the Centre of the aircraft's fuselage. Air entering these intake ducts must be turned through two curves (of opposite sign) before reaching the compressor face. Such a configuration results in an S-shaped air intake duct and therefore the engine performance becomes a strong function of the uniformity and direction of the inlet flow and these parameters are primarily determined by duct curvature.

This chapter intends to present a review of the flows in curved ducts and S-shaped ducts. Discussion is based on the Flow Separation, mechanism of total pressure loss and duct's exit flow conditions.

II. LITERATURE REVIEW

The total pressure distribution was represented on the S-duct exit and the thickened boundary layer along the outside wall of the second bend. The boundary layer near that wall to thicken rapidly due to enhanced entrainment and accumulate into a region of low momentum fluid. Another variant is due to the combined effects of centrifugal forces and radial pressure gradient in S-duct flows. Due to the increasing cross sectional area, a stream-wise adverse pressure gradient is also present. The combined effects may result in increased flow non-uniformity

and total pressure loss at the duct exit as compared to a uniformed cross sectioned S-duct [1, 5]. Blowing and vortex generators are used to energize low momentum of fluid near the separation point to overcome adverse pressure gradient [11].

The development of longitudinal vortices near the wall is accompanied by the rapid thickening of the boundary layer at the outside wall of the second bend. Since a favorable longitudinal pressure gradient exists on the outside wall of the second bend, the flow near this wall is accelerating and hence these longitudinal vortices could undergo " vortex stretching" , thus intensifying vorticity. This causes the boundary layer near that wall to thicken rapidly due to enhanced entrainment and accumulate into a region of low momentum fluid. large scale, vertical structures exist along the outside wall of the second bend in both the circular [4, 12].

Flows can be used by flow visualization only and in a Dean number range of 25 to 350. Their results show that Dean vortices formed at De = 101, 151, 201 and 252 and at a turning angle of about 180^0 in the first bend. These vortices continue to grow until 225^0 within the first bend and with increasing asymmetric structure for the higher De 201, while the vortices stay relatively symmetric for lower De of 101 and 151. Upon entering the second bend, the curvature of the outer and inner wall changes and the direction of the centrifugal force also changes accordingly. At 45^0 there still exist some remnants of the Dean vortices on the inner wall of the second bend that was generated on the outer wall of the first bend. Flows at higher De > 200 seem to display complex and asymmetrical structures in the second bend. The improvements in performance of S-shaped ducts are thus a reduction in flow distortion at the duct exits, maximizing the flow rate and hence minimizing the total pressure losses and elimination of flow separation if it is present [5]. Separation control flow can be done by flow control devices which are placed on the side walls of the S-duct and slightly upstream of the separation point so that when Vortex generators " locally" mix the high momentum fluid in the free stream with the low momentum fluid near the wall and thus energies the boundary layer to suppress flow separation [6].

Studies have done at the inlet of the duct, the high and low pressure side walls are respectively at the outer wall and inner wall of the first bend. The high and low pressure side changes in the second bend to reflect the change in duct curvature. The observation on swirl development in S-duct is generally true for both circular and non-circular geometry [7].

The marker-and-cell method is employed to allocate the parameters on the staggered mesh, and static pressure is calculated using the artificial compressibility approach. The effect of centrifugal force due to the curvature of the duct and the opposing effects of the first and second normal stress difference on the flow field are investigated. Based on the relations, the performance mechanism of centrifugal force and normal stress differences on the generation of secondary flows is considered [9].

Many numerical investigation for examining the secondary vortex motion and associated heat transfer process in fluid flow through curved passages taken place. For developing laminar fluid flow through curved rectangular ducts, the analysis performs a detailed parametric study involving the contours of helicity and outer duct wall pressure gradient for a range of flow rates, duct aspect ratios, duct flow curvatures and external wall heat fluxes. The flow conditions leading to hydrodynamic instability and Dean Vortex generation in curved passages are carefully analyzed, identifying the flow and geometrical parametric influences. Active interaction of buoyancy force on fluid motion

arising from wall heating is considered where aspects of boundary layer separation is used in recognizing thermal enhancement due to secondary flow [14].

It has been quoted that 0.4Umversus 0.15Um and 0.16Um versus 0.12Um for the corresponding thick and thin boundary layer cases. However, the details in flow topology within the second bend are dependent on whether flow separation is present. An increase in inlet boundary layer thickness led to a corresponding decrease in boundary layer thickness along the outer wall of the second bend. It has been also found that increasing inlet boundary layer led to a reduction in separation region in their S-duct study. The above review has concentrated mainly on S-duct with limited turning angle at relatively high Re (or De) where Dean vortices are not present[10, 15].

The vortex patterns of the secondary flow in a curved duct of square cross-section are numerically investigated. The flow is driven by the axial pressure gradient as well as the walls rotation of the duct except the outer wall around the center of curvature. When the rotation is in the same direction as the negative pressure gradient, the secondary flow shows complicated multiple patterns, which consists of two-vortex, four-vortex, eight-vortex or even non-symmetric secondary flow pattern [17].

III. RESULTS AND DISCUSSION

The optimum aerodynamic performance of S-shaped ducts (or aircraft air-intake ducts) demands that a relatively uniform flow with a smallest possible pressure loss. These requirements naturally lead one to consider the use of traditional flow control devices like vortex generators, blowing jets. Passive devices like vortex generators placed on the side wall eliminate flow separation if it is present. They "locally" mix the high-momentum fluid in the free stream with low-momentum fluid near the wall and thus suppress flow separation. In contrast to the passive means of flow control, blowing jets and vortex generator jets are active flow control devices for flow separation control, whereby mass addition near the separation point energizes the low momentum fluid close to the wall to overcome the adverse pressure gradient. To study the effects of flow control in square cross sectioned S-duct, vortex generator flow control method was studied In this Chapter, the relative merit of vortex generators on the flow in a square cross sectioned S-duct. Suppression of flow separation, reduction of total pressure loss, and flow uniformity at duct exit are the chosen criteria. Investigation of (S-duct Fig: 1) has been carried out with help of FLUENT, a CFD tool to simulate the Effect of pressure is studied. The present work is conducted at higher *Re*=4.73x10^{4}and1.47x10^{5}and with square cross-sectioned, S- shaped ducts with sharper bends and larger turning angle. The geometry is made in solid works and imported on Ansys software for analysis. After analysis on FLUENT following graphs are plotted.

Case 1: Study of 3D S-Shaped Duct:

Mesh Independency Study:

The grid independency is studied for the k-ε model employing four size of grid to examine the sensitivity of grid. As we get result in the third column that is fine mesh size is independent of grid that's the optimum grid.

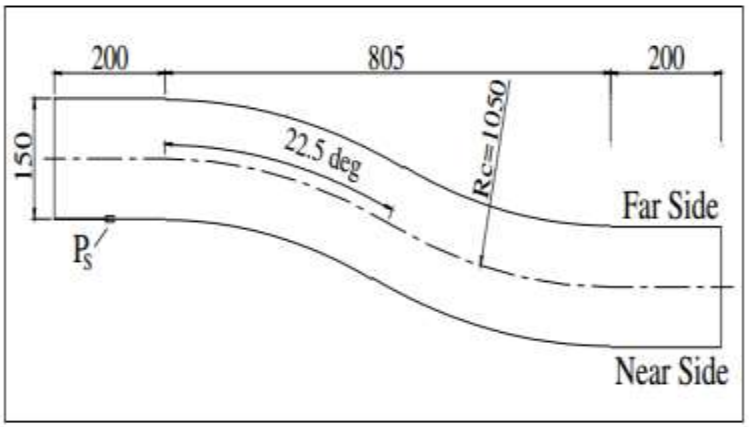

Fig: 1 S-duct configuration

Table: 1 Grid independency chart

	Maximum cell squish	**Maximum aspect ratio**	**Pressure and static pressure (min and max.)**	**Pressure and pressure coefficient**
coarse	5.05561×10^{-2}	2.03094	-1.37609, 3.683053	-2.246697, 6.013155
medium	6.5253×10^{-2}	2.16342	-1.553137, 3.96047	-2.535753, 6.466074
fine	9.28082×10^{-2}	2.18632	-1.585209, 4.26690	-2.5881, 6.966368
Mesh with sizing	9.28082×10^{-2}	2018632	-1.585209, 4.26690	-2.5881, 6.966368

On the study of 3d s-shaped duct we found that from Fig.2 and Fig.3 i.e. contour of static pressure there are two low pressure zones are create on the duct one at near side wall of the 1st bend and other on the far side wall of the second bend. On these two pocket of the bend there is a flow separation which is clearly seen by the Fig. no.4 i.e. contour of velocity vector. For suppressing this flow separation we can use different flow control techniques. From Fig. 2 and Fig. 3 it is clearly seen that the contour of static pressure is same for both the Reynolds number only there is difference in magnitude. Fig. 5 shows that the plot of static pressure vs. position.

Study of 3D S-Shaped Duct with Flow control Techniques:

Different flow control Techniques for improving the performance of S-Duct.

- Vortex generator

1. Study of 3D S-Shaped Duct with vortex generator:

Vortex generators " locally" mix the high momentum fluid in the free stream with the low momentum fluid near the wall and thus energies the boundary layer to suppress flow separation.

Graphs of Static Pressure Contours:

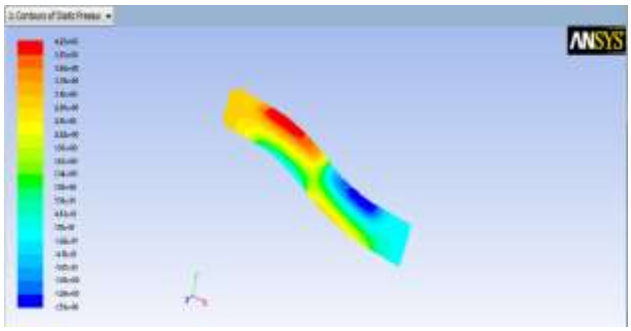

Fig: 2 Contour of Static Pressure at *Re*=4.73x10^4

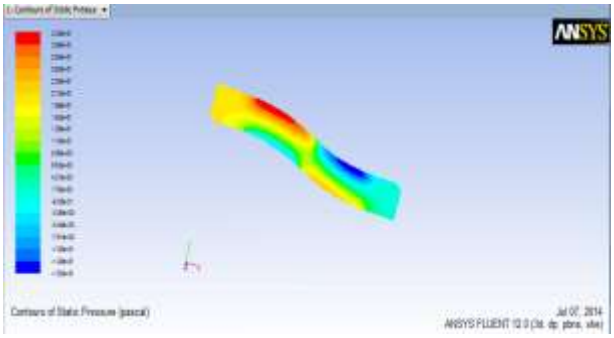

Fig: 3 Contour of static Pressure at *Re*=1.47x10^5

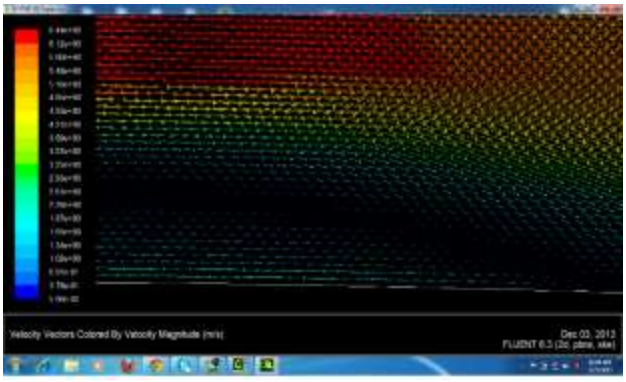

Fig: 4 Velocity vector showing flow separation.

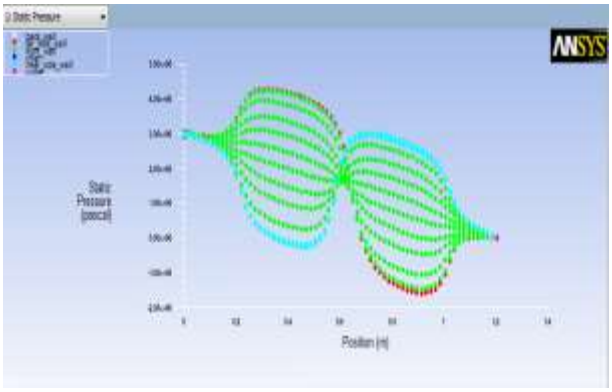

Fig: 5 Graph of static pressure v/s position

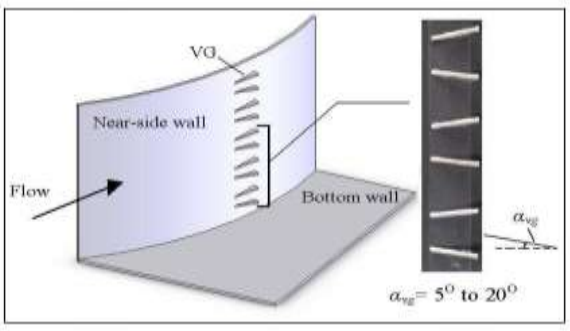

Fig: 6 Vortex generator on near side wall

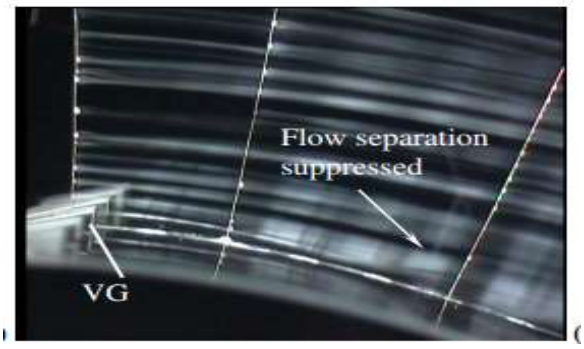

Fig: 7 Shows flow separation and suppressed flow [13]

On the study of 3d S-shaped duct with flow control technique i.e. with vortex generator we found that from Fig.9 and Fig.10 i.e. contour of static pressure there are no low pressure zones are create on the duct one at near side wall of the 1st bend and other on the far side wall of the second bend as found from the analysis from bare duct. From Fig. 9 and 10 it is clearly seen that the contour

of static pressure is same for both the Reynolds number only there is difference in magnitude. Fig 11 shows that the plot of static pressure vs. position .the trend obtained from Fig. 11 is clearly matched with the Fig. 13 i.e. practically result obtained by the Thye,N. Y., 2009.now from the different values obtained from the pressure graph we calculate value of Cp at different point of the duct which is shown on the Table no 2. Fig.12 shows graph obtained Cp v/s s/d by simulation which is matched by the practical result.

From the above simulation results following tables and graphs are plotted for surface pressure distribution Cp and total pressure loss coefficient.

Effects of Flow Control Devices:

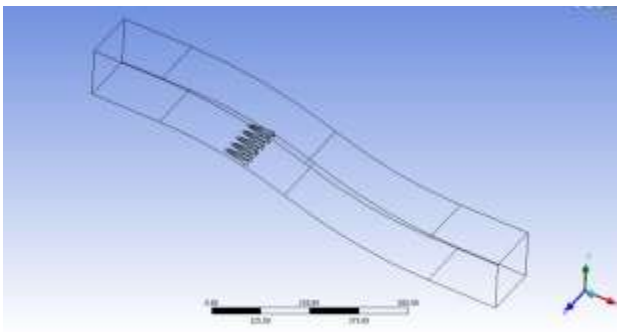

Fig: 8 S-duct with vortex generator

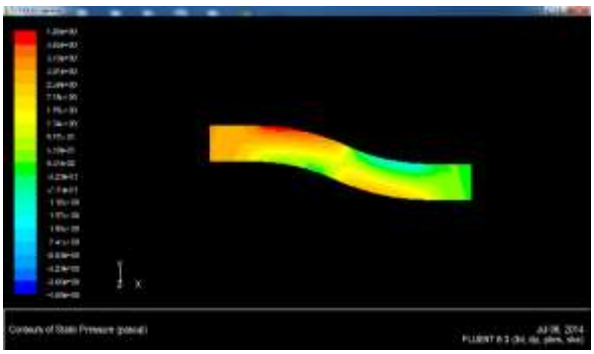

Fig: 9 Contour of static pressure v/s position for *Re*=4.73x1

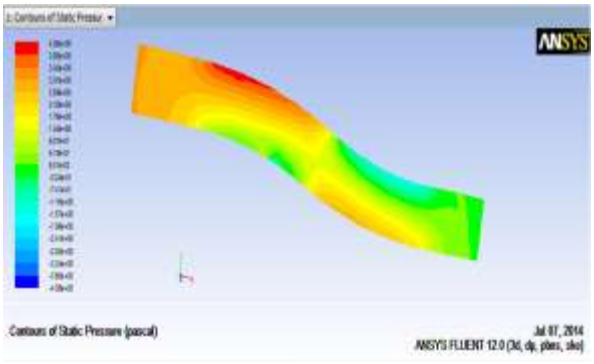

Fig: 10 Contour of static pressure v/s position for *Re*=1.47x10

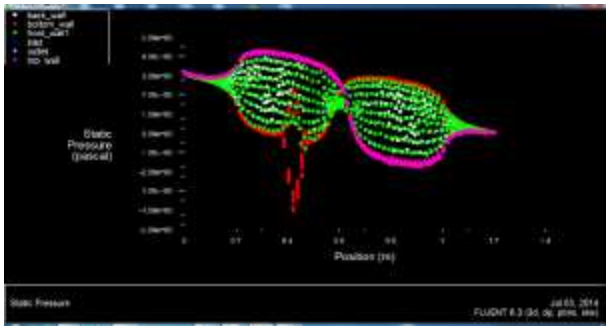

Fig: 11 Plot of static pressure v/s position

2. Table of surface pressure distribution on the side wall (far side wall and near side wall) for bare duct and duct with vortex generator at Re=4.73x10^4

Table.2: Surface pressure distribution on the side wall at *Re*=4.73x10^4

S/D	Cp far Side (bare)	Cp far Side (vg)	Cp Near Side (bare)	Cp Near Side (vg)
0	0.21	0.2	-0.3	-0.35
0.25	0.3	0.3	-0.45	-0.47
0.5	0.35	0.35	-0.52	-0.7
0.75	0.43	0.44	-0.55	-1
1	0.3	0.35	-0.45	-0.7
1.25	0.3	0.3	-0.5	-0.58
1.5	-0.25	-0.1	-0.5	-0.2
1.75	-0.4	-0.25	-0.2	0
2	-1.1	-0.8	-0.2	0.2
2.25	-1	-0.9	-0.01	0.25
2.5	-1.05	-0.9	0	0.25
2.75	-0.9	-0.8	0	0.25
3	-0.9	-0.7	0	0.15
3.25	-0.5	-0.6	0.2	0.2
3.5				

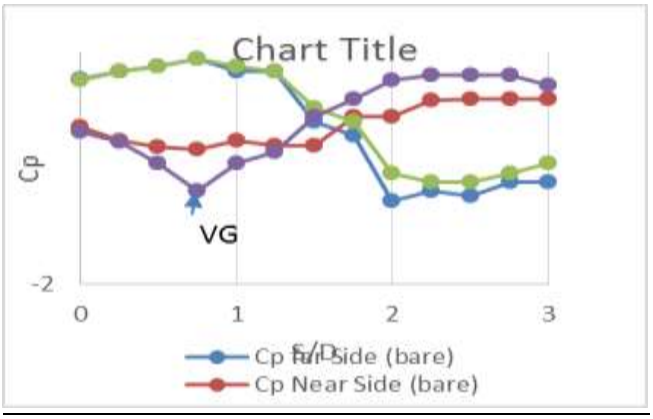

Fig: 12 Surface pressure distribution on the side wall at *Re*=4.73x10^4

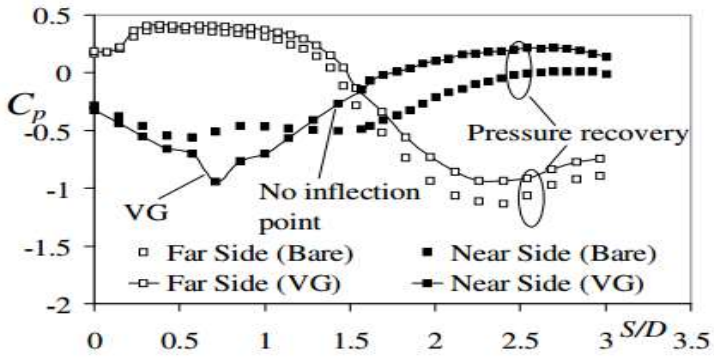

Fig: 13. Graph of Cp v/s S/D obtained practically by Thye, N. Y [13] at *Re*=4.73x10^4

From above chart it is clearly seen that there is no point of inflection in case of duct with vortex generator as compare to bare duct so it can be concluded from above chart that flow separation is suppressed by use of flow control device i.e. vortex generator.

From Fig.12 and Fig.14 it is seen that there is no point of inflection in case of duct with vortex generator as compare to bare duct so it can be concluded from above chart that flow separation is suppressed by use of flow control device i.e. vortex generator and the pattern obtained by simulation is similar to the graph of Cp vs S/D obtained practically by Thye, N.Y. i.e.Fig.13.

3. Table of surface pressure distribution on the side wall (far side wall and near side wall) for bare duct and duct with vortex generator at Re= 1.47x10^5

Table 3: surface pressure distribution on the side wall at *Re*=4.73x10^4

S/D	Cp far Side (bare)	Cp far Side (vg)	Cp Near Side (bare)	Cp Near Side (vg)
0	0.3	0.3	-0.35	-0.35
0.25	0.3	0.3	-0.45	-0.47
0.5	0.45	0.45	-0.65	-0.65
0.75	0.43	0.44	-0.55	-0.9
1	0.4	0.4	-0.6	-0.65
1.25	0.3	0.3	-0.5	-0.55
1.5	-0.1	-0.05	-0.05	0
1.75	-0.3	-0.25	0.28	0.3
2	-0.65	-0.6	0.25	0.25
2.25	-0.92	-0.9	0.35	0.4
2.5	-0.9	-0.9	0.35	0.3
2.75	-0.82	-0.8	0.25	0.25
3	-0.7	-0.7	0.25	0.2
3.25	-0.5	-0.6	0.2	0.2
3.5				

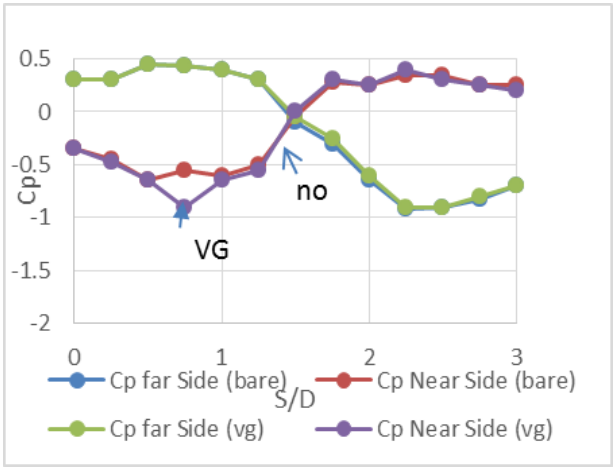

Fig: 14 surface pressure distribution on the side wall at *Re*=1.47x10^5

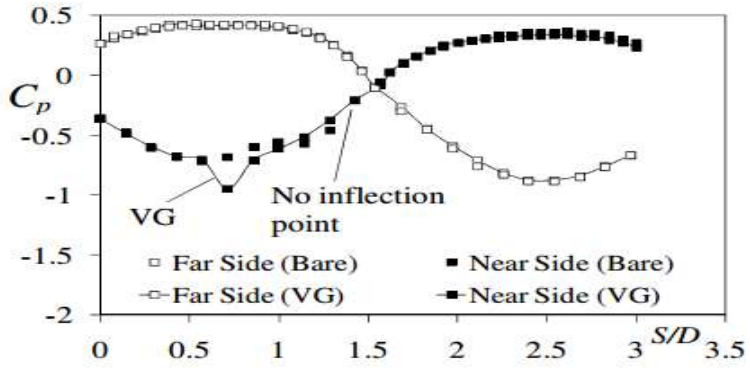

Fig: 15. Graph of Cp v/s S/D obtained practically byThye, N. Y [13] *Re*=1.47x10^5

From Fig.12 and Fig.14 it is seen that there is no point of inflection in case of duct with vortex generator as compare to bare duct at Re=1.47 X 10^5 so it can be concluded from above chart that flow separation is suppressed by use of flow control device i.e. Tangential Blowing and the pattern obtained by simulation is similar to the graph of Cp vs S/D obtained practically by Thye, N.Y. i.e. Fig. 15.

Total Pressure Loss:

Table 4: Total pressure loss coefficient with respect to Reynolds number for bare and vortex generator duct.

Sr. No	**Total pressure loss coefficient**	**Reynolds number 4.73x10^4**		**Reynolds number 1.47x10^5**	
		simulation	Experimental[14]	Simulation	Experimental[14]
1.	Bare Duct	0.2	0.24	0.25	0.2
2.	VG	0.115	0.2	0.12	0.13
3.	Tangential Blowing Cm=0.12	0.15	0.16	0.15	0.14
4.	Tangential blowing Cm=0.045	0.12	0.13	0.125	0.12

Variation of total pressure loss coefficient 5^0 angle for VG configuration at Re = 4.73x10^{4}and Variation of total pressure loss coefficient at 5^0 angle for VG configuration at Re = 1.47x10^5 it is found that there is reduction in total pressure loss coefficient by using vortex generator .As total loss coefficient is 0.25 and 0.2 for the bare duct for respective Reynolds number. In case of vortex generator it is 0.115 For Re=4.73x10^4. For Reynolds number 1.473x10^{5}for vortex generator it is 0.2.

IV. CONCLUSION

The optimum aerodynamic performance of S-shaped ducts (or aircraft air-intake ducts) demands that a relatively uniform flow with a smallest possible pressure loss. The contour of static pressure obtained from simulation of bare Duct, shows two low pressure zones are developed on the duct, one at near side wall of the 1st bend and other on the far side wall of the second bend. There is a flow separation in these two pockets of the bend which is clearly seen on the contour of velocity vector (Fig. 6).As we use two Reynolds number the effect is same, only difference in magnitude observed. Flow control techniques namely Vortex generator is used to suppress the flow separation there why reducing total pressure loss. The effectiveness of VGs to control flow separation, reduce total pressure loss is studied. The graph of Cp vs S/D (Fig.12) of simulation shows no point of inflection i.e. there is no flow separation on these walls. There is also reduction in total pressure loss coefficient by using vortex generator shown in table 4. As total loss coefficient is 0.25 and 0.2 for the bare duct for respective Reynolds number. In the case of vortex generator it is 0.115 and 0.2 for respective Reynolds number. The method vortex generator was shown to be effective in suppressing flow separation and reducing total pressure loss. Therefore the results indicates competing parameters for improving the performance of flow in S-ducts.

V. REFERENCES

[1] B.H Anderson and J. Gibb, Vortex-Generator Installation Studies on Steady-State and Dynamic Distortion, Journal of Aircraft, 35(4), (1998), 513-520.
[2] B.H Anderson, D.R. Reddy and K. Kapoor, Study on Computing Separating Flows Within a Diffusing Inlet S-duct, Journal of Propulsion and Power, 10(5), (1994), 661-667.
[3] B.H Anderson, A.M.K.P Taylor, J.H Whitelaw and M. Yianneskis. Developing Flow in S shaped Ducts. In: Proceeding of Second Symposium on the Application of LDA to Fluid Mechanics, Lisbon, Portugal, 4.2,1982, 17.
[4] P. Bansod and P.Bradshaw, The Flow in S-Shaped Ducts, Aeronautical Quarterly, 23, (1972), 131-140.
[5] K.C Cheng and L. Shi, Visualizations of Developing Secondary Flow and Measurements of Velocity Profiles in a Curved Square Duct with and without an Offset Bend. In: Flucome '91, 3rd Triennial International Symposium on Fluid Control, Measurement, and Visualization, San Francisco, USA, (1991), 415-422.
[6] M.Gad-el Hak and D.M Bushnell, Separation Control: Review, Transactions of ASME: Journal of Fluid Engineering, 113(1), (1991), 5-30.
[7] R.W Guo and J. Seddon , The Swirl in an S-duct of Typical Air Intake Proportions, Aeronautical Quarterly, 34(2),1983, 99-129.
[8] B.J. Kitchen and J.M. Jr. Bowyer, Towards the Optimization of a Non-diffusing Two Dimensional, S-shaped Duct, In: Forum of Turbulent Flows, ASME Fluid Engineering Division FED, San Diego, USA, 76, (1989), 85-92.
[9] M. Norouzia, M.H. Kayhani, C.Shu, M.R.H. Nobari et al. , Flow of second-order fluid in a curved duct with square cross-section,Journal Non-Newtonian Fluid Mech.165, (2010) ,323–339.
[10] J.Rojars, J.H Whitelaw, and M. Yianneskis, Developing Flows in S-shaped Diffusers Part I: Square to Rectangular Cross Section Diffuser, NASA Contractor Report 3631, (1983), 50.
[11] R.K. Sullerey, and A.M. Pradeep, Effectiveness of Flow Control Devices on S-Duct Diffuser Performance in the Presence of Inflow Distortion, International Journal of Turbo and Jet-Engines, 19(4), (2002), 259-270.
[12] A.M.K.P Taylor, J.H. Whitelaw and M. Yianneskis, Developing Flow in S-shaped Ducts 2: Circular Cross-section Duct, NASA Contractor Report 3759, 1984, 60.
[13] N.Y.Thye. A Thesis, Doctor of Philosophy, National University of Singapore, 2009.

[14] T. Chandratilleke Tilak, NimaNadim, Ramesh Narayanaswamy et al , Vortex structure-based analysis of laminar flow behavior and thermal characteristics in curved ducts, International Journal of Thermal Sciences 59, (2012), 75e86.
[15] J.H.Whitelaw and S.C.M Yu, Turbulent Flow Characteristics in an S-shaped Diffusing Duct, Flow Measurement and Instrumentation, 4(3),1993a, 171-179.
[16] J.H Whitelaw and S.C.M Yu, S.C.M. Velocity Measurements in an S-shaped Diffusing Duct, Experiments in Fluids, 15(3-4), 1993b, 364-367.
[17] Wu Xiaoyun , Sangding Lai, Kyoji Yamamoto, Shinichiro Yanase et al, Vortex Patterns of the Flow in a Curved Duct, ICSGCE 2011.
[18] S.C.M Yu and E.L.Goldsmith. Some Aspects of the Flow in S-shaped Diffusing Ducts, Aeronautical Journal, 98(978), 1994, 305-310.

